Journal of Applied Sciences

ISSN 1812-5654

Journal of Applied Sciences 7 (9): 1249-1259, 2007
ISSN 1812-5654

Study of an Engineering Mixed Contact: Part I-Theoretical Analysis

Yongbin Zhang
Zhejiang Jinlei Electronic and Mechanical Co. Ltd., Zhejiang Province,
Peoples Republic of China

Abstracts: The present study presents theoretical analysis of an engineering mixed lubrication contact in one-dimensional case between a deformable plane of regular roughness and an ideally smooth rigid plane. The roughness of the plane, respectively take the forms of triangle and truncated triangle ridges which are evenly distributed on the plane surface. The rough plane is assumed as elastic-plastic. The contact between the tip of the ridge on the plane and the other smooth plane is assumed as in dry contact or oxidized chemical boundary layer contact, while the regions between other parts of the ridge and the smooth plane are, respectively in physical adsorbed boundary layer contact and continuum film hydrodynamic contact. The lubricant in the continuum film hydrodynamic contact is assumed as Newtonian. The whole contact between these two planes is obtained by periodically distributing the ridge on the plane. Theoretical analysis are developed for this mode of contact, respectively for triangle and truncated triangle surface ridges for wide operational parameters when the plane ridge, respectively undergoes elastic and plastic deformations and the hydrodynamic contact areas between the planes are varied. The present study demonstrates the theoretical analysis. In the following parts will be demonstrated the results obtained from the present analysis.

Key words: Engineering mixed contact, dry contact, oxidized chemical boundary layer, physical adsorbed boundary layer, hydrodynamic contact

INTRODUCTION

Mixed lubrication contact in mechanical engineering was conventionally defined as the hydrodynamic contact in which the contact surface roughness effect is considerable. The analysis of this contact should incorporate the contact surface roughness effect. In the past time, the type of the analysis of mixed lubrication contact can be classified as two kinds i.e., stochastic approach and deterministic approach. Stochastic approach studies the statistical effect of the contact surface roughness in mixed lubrication contact by considering the stochastic and random properties of the contact surface roughness. The stochastic approach to mixed lubrication contact only needs a few characterization parameters of the contact surface roughness which are the same for a batch of hydrodynamic components. It can give the average hydrodynamic pressure and the average hydrodynamic film thickness in mixed lubrication contact for a batch of rough hydrodynamic components which have the same values of the contact surface roughness characterization parameters. However, since the contact surface roughness in mixed lubrication contact practically essentially causes the time dependent i.e., transient performance of the contact, the stochastic approach has the shortcoming of being unable to give the instant film pressure and thickness distributions in the contact, the variations of the film pressure and thickness with time and the characteristic values of both the film pressure and thickness during these variations such as the maximum hydrodynamic pressure, the local fluid cavitation (i.e., the minimum hydrodynamic pressure), the maximum hydrodynamic pressure gradient and the minimum hydrodynamic film thickness, which are important for the failures of the mixed lubrication contact. Therefore, the stochastic mixed lubrication contact results are not able enough to describe the performance of the contact. It is mainly used in determination of the condition of this kind of contact. The studies of mixed lubrication contact in the references of Christensen and Tonder (1969), Patir and Cheng (1979) and Hughes and Bush (1993) belong to this type of approach.

To give more detailed and precise mixed lubrication contact results and to better describe the performance of this contact, the deterministic approach was used. In the past time, the contact surface roughness was either artificially defined or measured for one defined couple of hydrodynamic components when applying the deterministic approach to mixed lubrication contact. The steady-state or transient results for mixed lubrication contacts were usually numerically solved for a given operating condition based on this contact surface roughness by the deterministic approach. These results give the real-time hydrodynamic film pressure and thickness during the operation. Therefore, these results detailed and precisely describe the performance of mixed lubrication contact for a given operating condition.

The deterministic approach is more capable of exploring the mechanism of the contact surface roughness effect in mixed lubrication contact than the stochastic approach. In the past time, it was popularly used in the mixed lubrication contact analysis. The studies in the references of Goglia *et al.* (1984) and Lubrecht *et al.* (1988) and Greenwood and Johnson (1992) belong to this type of approach.

Before 1990s, the theoretical analysis of mixed lubrication contact was mainly limited to the study of the mixed lubrication contact where the hydrodynamic film was fully distributed in the whole contact and the hydrodynamic film was relatively thick and thus continuum across the film thickness. In Jiang *et al.* (1999) presented an analysis of mixed lubrication contact considering the direct contact between the coupled surface asperities. Their study was substantially progressive than the earlier theoretical study of mixed lubrication contact. In Holmes *et al.* (2003) pointed out that the direct surface asperity contact should not occur in the way Hu and Zhu (2000) described in their analysis (Holmes *et al.*, 2003), which was very similar to the analysis by Jiang *et al.* (1999). They suggested that fluid side leakage have a predominant effect on the direct asperity contact occurrence in this contact. However, Zhang (2005a) pointed out that the direct surface asperity contact may be not directly caused by fluid side leakage but directly caused by the surface pressure effect.

In the review of the research on mixed lubrication contact, Zhang (2004a) classified the modes of mixed lubrication contact in the theoretical analysis in the past time as three kinds i.e., the classical mode of mixed lubrication contact, the modern mode of mixed lubrication contact and the future mode of mixed lubrication contact. The classical mode of mixed lubrication contact refers to the contact where the hydrodynamic film is fully distributed in the whole contact area and the hydrodynamic film is relatively thick and thus continuum across the film thickness. The modern mode of mixed lubrication contact refers to the contact where the hydrodynamic film between the rough contact surfaces is molecularly thin on some separate locations of the contact, while in the other zones of the contact the hydrodynamic film is relatively thick and thus continuum across the film thickness. The future mode of mixed lubrication contact refers to the contact where the physical adsorbed boundary layer contact may occur on some separate locations of the whole contact, at the same time the oxidized chemical boundary layer contact and the fresh metal to metal dry contact between the opposing asperities of the contact surfaces may occur, respectively on some other separate locations of the whole contact, while in the other zones of the whole contact the hydrodynamic film is relatively thick and thus continuum across the film thickness. Zhang (2004a) pointed out that the future mode of mixed lubrication contact is the most advanced. These arguments were also mentioned in his other papers (Zhang, 2006a,b).

The present study presents an analysis of an engineering mixed lubrication contact, which belongs to the future mode of mixed lubrication contact. The analyzed contact is one-dimensional. One contact surface is taken as the rough contact surface where the triangle or truncated triangle ridges are periodically imposed. This contact surface is treated as elastic-plastic. The other contact surface is taken as ideally smooth and rigid. Dry contact or oxidized chemical boundary layer contact occur between the tip of the ridge and the smooth plane. Between other parts of the ridge and the smooth plane, respectively occur physical adsorbed boundary layer contact and continuum film hydrodynamic contact, according to the formed film between the mated contacts. During the loading of the contact, the surface ridge is compressed and undergoes elastic or plastic deformations and the direct contact area between the two contact surfaces formed on the tip of the ridge is increased; The physical adsorbed boundary layer contact area and the continuum film hydrodynamic area between the two contact surfaces are also, respectively varied with the loading of the contact. The load partitions in different types of contact areas between the two contact surfaces are also changed with the operating condition. This mode of contact is believed to follow the engineering contact, according to the experiments (Begelinger and Gee de, 1974, 1976; Tabor, 1981). In the present study is presented analysis of this contact. In the following parts will be presented the results obtained from the present analysis for this contact.

MODEL

The analyzed contact models are, respectively shown in Fig. 1a and Fig. 1b. In Fig. 1a and Fig. 1b, the upper contact surface is rough, elastic-plastic and moving with the speed u; The lower contact surface is ideally smooth, rigid and stationary. In Fig. 1a and b, the contact surface ridges are, respectively isosceles triangle and isosceles truncated triangle both with the half ridge angle θ and their initial heights both are h_0. In these two figures, the initial wavelength of the contact surface roughness is l_w and L is the initial contact width of the rough surface (before loading).

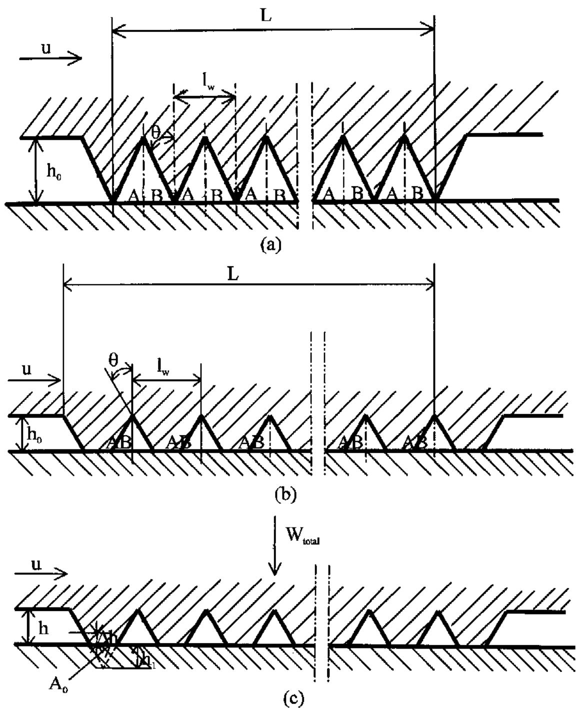

Fig. 1: Analyzed contact. (a) The surface ridge is isosceles triangle; (b) The surface ridge is isosceles truncated triangle and (c) Example of the contact under loading

In Fig. 1, when the contact is loaded and then the ridge and the ideally smooth plane are in direct contact carrying a load, the ridge is compressed and undergoes elastic or plastic deformations; In the zone A of the contact, the hydrodynamic pressure is built up, while in the zone B of the contact, the fluid is cavitated and the hydrodynamic pressure vanishes. The load of the contact is carried by both the ridge-plane direct contact and the hydrodynamic lubricated area formed in the contact. Figure 1c schematically shows an example of the analyzed contact under loading.

In the following sections will be, respectively derived the load-carrying capacities of the ridge-plane direct contact area and the hydrodynamic lubricated area in the present model when the contact surface ridge is, respectively isosceles triangle and isosceles truncated triangle.

ANALYSIS

Ridge elastic-plastic deformations

For isosceles triangle surface ridge

Elastic deformation

Basic equations: For isosceles triangle surface ridges as shown in Fig. 1a, according to the theory of elasticity (Timoshenko and Goodier, 1951), the area of the elastic contact formed between a single ridge and the ideally smooth rigid plane is expressed as:

$$A = k\,F^{1/2} \tag{1}$$

where F is the force exerted on the whole area of this contact and k is constant.

Differentiating Eq. 1 gives that:

$$\Delta A = \frac{1}{2} k\,F^{-1/2} \Delta F \tag{2}$$

While, according to Fig. 1c, the variation of the direct surface contact area between a single ridge and the smooth plane is expressed as:

$$\Delta A = -2l \frac{\Delta h}{\cos\theta} \tag{3}$$

where h is the film thickness between the root of the ridge and the smooth plane and l is the contact length of the ridge.

Substituting Eq. 2 into Eq. 3 yields:

$$\Delta h = -\frac{k\cos\theta\,\Delta F}{4lF^{1/2}} \tag{4}$$

Integrating Eq. 4 gives:

$$h = -\frac{k\cos\theta\,F^{1/2}}{2l} - c_0 \tag{5}$$

where c_0 is an integral constant. From the boundary condition $h|_{F=0} = h_0$, it is solved from Eq. 5 that $c_0 = -h_0$. Thus, Eq. 5 is re-expressed as:

$$h = -\frac{k\cos\theta\,w_{A0,single}^{1/2}}{2l^{1/2}} + h_0 \tag{6}$$

where $w_{A0,single}$ is the load per unit contact length on the direct surface contact area between a single ridge and the smooth plane and $w_{A0,single} = F/l$.

Let $w_{A0,single} = w_{max,e}$ when $h = h_{cr,e}$; Here, $h_{cr,e}$ is the (critical) value of the film thickness h when the ridge is in the maximum elastic deformation and $w_{max,e}$ is the maximum load on the direct surface contact area between a single ridge and the smooth plane when the ridge undergoes elastic deformation. Therefore, when $h_{cr,e}<h<h_0$, the ridge is in elastic deformation; While, when $h \le h_{cr,e}$, the ridge is in plastic deformation.

From the boundary condition $w_{A0,single}|_{h = hcr,e} = w_{max,e}$, it is solved from Eq. 6 that:

$$\frac{k}{l^{1/2}} = \frac{2(h_0 - h_{cr,e})}{w_{max,e}^{1/2}\cos\theta} \qquad (7)$$

Thus, when $h_{cr,e}<h<h_0$ in the condition of the ridge elastic deformation, the film thickness expression is:

$$h = h_0[1 - (\frac{w_{A0,single}}{w_{max,e}})^{1/2}] + h_{cr,e}(\frac{w_{A0,single}}{w_{max,e}})^{1/2} \qquad (8)$$

Integrating Eq. 3 and using the boundary condition $A|_{h=h_0} = 0$ gives the formed direct surface contact area between a single ridge and the smooth plane as follows:

$$A = \frac{2l(h_0 - h)}{\cos\theta} \qquad (9)$$

In the present analysis, the average pressure p_{av} formed on the direct surface contact area between the ridge and the smooth plane is used for judging whether the ridge-plane direct contact is in elastic or plastic deformations. When $p_{av}<p_y$, the ridge-plane direct contact is in elastic deformation; While, when $p_{av} = p_y$, it is in plastic deformation; Here, p_y is the compressive yielding strength of the ridge. According to this principle, on the inception of the ridge plastic deformation, there is:

$$\frac{w_{max,e}\cos\theta}{2(h_0 - h_{cr,e})} = p_y \qquad (10)$$

Determine the parameters $w_{max,e}$ and $h_{cr,e}$: Solving the coupled Eq. 7 and 10 gives the expressions, respectively for $w_{max,e}$ and $h_{cr,e}$ as follows:

$$w_{max,e} = (p_y \frac{k}{l^{1/2}})^2 \qquad (11)$$

$$h_{cr,e} = h_0 - \frac{p_y\cos\theta}{2}(\frac{k}{l^{1/2}})^2 \qquad (12)$$

Plastic deformation: When the ridge undergoes plastic deformation, the variation of the direct surface contact area between a single ridge and the smooth plane is expressed as:

$$\Delta A = \frac{\Delta F}{p_y} \qquad (13)$$

where ΔF is the variation of the force exerted on the whole area of this contact.

Substituting Eq. 3 into Eq. 13 and rearranging gives:

$$\frac{\Delta w_{A0,single}}{\Delta h} = -\frac{2p_y}{\cos\theta} \qquad (14)$$

Integrating Eq. 14 gives the following relation equation:

$$h = c_1 - \frac{w_{A0,single}\cos\theta}{2p_y} \qquad (15)$$

where c_1 is an integral constant. By using the boundary condition $W_{A0,\,single}\,|h = h_{cr,e} = W_{max,e}$, it is solved from Eq. 15 that $c_1 = h_{cr,e} + W_{max,e}\cos\theta/(2p_y)$ Thus, when $h \le h_{cr,e}$, in the condition of the ridge plastic deformation, the film thickness expression is:

$$h = h_{cr,e} + \frac{(w_{max,e} - w_{A0,single})\cos\theta}{2p_y} \qquad (16)$$

Based on Eq. 10 and 16 can actually be further simplified as:

$$h = h_0 - \frac{w_{A0,single}\cos\theta}{2p_y} \qquad (17)$$

It can be found that in the condition of the ridge plastic deformation, the average pressure formed on the ridge-plane direct contact area is always equal to the compressive yielding strength of the ridge p_y.

Contact stiffness: In the condition of the ridge elastic deformation, the contact stiffness of the direct surface contact area between a single ridge and the smooth plane is obtained as:

$$\frac{\Delta w_{A0,single}}{\Delta h} = \frac{4p_y(h_0 - h)}{(h_{cr,e} - h_0)\cos\theta} \qquad (18)$$

In the condition of the ridge plastic deformation, this stiffness is expressed as Eq. 14.

Contact surface temperature rise: Considering the frictional heating in the ridge-plane direct contact area is the main heat source of the whole mixed lubrication contact and the contact surface temperature rise is mainly represented by the temperature rise of the direct contact area between the ridge and the smooth plane, the temperature rise of the direct contact area between the ridge and the smooth plane due to the frictional heating is expressed as (Blok, 1937):

$$\Delta T = \frac{0.415f\ w_{A0,single}\sqrt{u\cos\theta}}{\sqrt{k_m \rho_m c_m (h_0 - h)}} \qquad (19)$$

where f is the friction coefficient of the ridge-plane direct contact area, k_m is the heat conduction coefficient of the rough surface, ρ_m is the density of the rough surface and c_m is the specific heat of the rough surface.

For isosceles truncated triangle surface ridge: The present study also studies the mixed lubrication performance when the isosceles triangle ridge on the rough plane is shaved in different degrees i.e., when the rough plane ridge is isosceles truncated triangle. The contact model for this case is shown in Fig. 1b. Contact analysis for the coupling of the isosceles truncated triangle surface ridge and the smooth plane shown in Fig. 1b is demonstrated as follows.

Elastic deformation

Basic equations: According to the theory of elasticity (Timoshenko and Goodier, 1951), the infinitesimal variation of the area of the direct contact between a single ridge and the ideally smooth rigid plane shown in Fig. 1 b which is elastic is expressed as:

$$\Delta A = \frac{k^2}{2}(k^2 F + A_{org}^2)^{-1/2}\Delta F \qquad (20)$$

where A_{org} is the initial direct contact area between a single ridge and the smooth plane and $A_{org} = 2b_0 l$ (b_0 is the initial half width of the direct contact between a single ridge and the smooth plane), F is the force exerted on the whole area of this contact, ΔF is its infinitesimal variation and k is same as shown in Eq. 1.

Substituting Eq. 3 into Eq. 20 and rearranging gives:

$$\Delta h = -\frac{k^2\cos\theta}{4l}(k^2 F + A_{org}^2)^{-1/2}\Delta F \qquad (21)$$

Integrating Eq. 21, using the boundary condition $h|_{F=0} = h_0$ and rearranging gives:

$$h = h_0 + b_0\cos\theta - [(\frac{\cos\theta}{2}\frac{k}{l^{1/2}})^2 w_{A0,single} + b_0^2\cos^2\theta]^{1/2} \qquad (22)$$

Similar as described earlier let $w_{A0,single} = w_{max,e}$ when $h = h_{cr,e}$. The definitions of $w_{max,e}$ and $h_{cr,e}$ are same as described above. Thus, when $h_{cr,e}<h<h_0$, the surface ridge undergoes elastic deformation; While, when $h \le h_{cr,e}$, the surface ridge undergoes plastic deformation.

From the boundary condition $w_{A0,single}|_{h=h_{cr,e}} = w_{max,e}$, it is solved from Eq. 22 that:

$$\frac{k}{l^{1/2}} = \frac{2}{\cos\theta}[\frac{(h_0 + b_0\cos\theta - h_{cr,e})^2 - b_0^2\cos^2\theta}{w_{max,e}}]^{1/2} \qquad (23)$$

Substituting Eq. 23 into Eq. 22 gives the film thickness expression in the condition of the ridge elastic deformation when $h_{cr,e}<h<h_0$ as follows:

$$h = h_0 + b_0\cos\theta - [\frac{(h_0 + b_0\cos\theta - h_{cr,e})^2 - b_0^2\cos^2\theta}{w_{max,e}} w_{A0,single} + b_0^2\cos^2\theta]^{1/2} \qquad (24)$$

Integrating Eq. 3 and using the boundary condition $A|_{h=h_0} = A_{org}$ gives the formed direct surface contact area between a single ridge and the smooth plane as follows:

$$A = \frac{2l}{\cos\theta}(h_0 - h + b_0\cos\theta) \qquad (25)$$

Using the same principles of judging the ridge elastic and plastic deformations as presented earlier on the inception of the ridge plastic deformation, there is:

$$\frac{w_{max,e}\cos\theta}{2(h_0 - h_{cr,e} + b_0\cos\theta)} = p_y \qquad (26)$$

Determine the parameters $w_{max,e}$ and $h_{cr,e}$: Solving the coupled Eq. 23 and 26 gives the expressions, respectively for $w_{max,e}$ and $h_{cr,e}$ as follows:

$$w_{max,e} = \frac{(p_y\frac{k}{l^{1/2}})^2 + \sqrt{(p_y\frac{k}{l^{1/2}})^4 + 16b_0^2 p_y^2}}{2} \qquad (27)$$

$$h_{cr,e} = h_0 + b_0\cos\theta - \frac{\cos\theta[p_y(\frac{k}{l^{1/2}})^2 + \sqrt{p_y^2(\frac{k}{l^{1/2}})^4 + 16b_0^2}]}{4} \quad (28)$$

Plastic deformation: Equation 13 through 16 are still valid for the isosceles truncated triangle surface ridge in the present analysis. Based on Eq. 26, when $h \le h_{cr,e}$, in the condition of the ridge plastic deformation, the film thickness expression can be further simplified as follows, according to Eq. 16:

$$h = h_0 + b_0\cos\theta - \frac{\cos\theta\, w_{A0,single}}{2p_y} \quad (29)$$

It can be found that for the present case, in the condition of the ridge plastic deformation, the average pressure formed on the ridge-plane direct contact area is always equal to the compressive yielding strength of the ridge p_y.

Contact stiffness: In the condition of the ridge elastic deformation, the contact stiffness of the direct surface contact area between a single ridge and the smooth plane for the present case is obtained as:

$$\frac{\Delta w_{A0,single}}{\Delta h} = \frac{4p_y(h - h_0 - b_0\cos\theta)(h_0 - h_{cr,e} + b_0\cos\theta)}{\cos\theta[(h_0 + b_0\cos\theta - h_{cr,e})^2 - b_0^2\cos^2\theta]} \quad (30)$$

In the condition of the ridge plastic deformation, this stiffness is expressed as Eq. 14.

Contact surface temperature rise: Similar as described earlier the temperature rise of the ridge surface in the direct contact area between the ridge and the smooth plane due to the frictional heating is derived as:

$$\Delta T = \frac{0.415f\, w_{A0,single}\sqrt{u\cos\theta}}{\sqrt{k_m\rho_m c_m(h_0 - h + b_0\cos\theta)}} \quad (31)$$

Lubricant film lubrication: Now here is analyzed the lubricant film lubrication occurring in the present mode of mixed lubrication. Figure 1a and b show that in the present modeled contact the lubricant film lubrication occurs in the zone A of the contact shown in these figures, while the fluid in the zone B of the contact is cavitated and no lubricant film pressure should be built there because of the divergent gaps between the contact surfaces formed there (Pinkus and Sternlicht, 1961). Figure 2a shows the geometry of the zone A of the present contact for both isosceles triangle and isosceles truncated triangle surface ridges when the contact is loaded.

In the present analysis, the half ridge angle θ is assumed as constant when the contact is loaded, the width (l_1) of the zone A shown in Fig. 2a is thus equated as l_1 = h tan θ and the film thickness h in Fig. 2a is varied with the load of the contact. Figure 2b more clearly shows an elementary cell of the zone A and its geometries in the present analysis. As Fig. 2b shows, the zone A of the present contact can actually be divided into two sub-zones, which are, respectively named as zone A_1 and zone A_2. In the zone A_1 occurs conventional hydrodynamic lubrication because of the relatively high lubricant film thickness and the continuum lubricant film lubrication there; While, in the zone A_2 occurs physical adsorbed layer boundary lubrication because of the very low lubricant film thickness and the physical adsorption and ordering of the lubricant film to the contact surfaces there. Therefore, in the present mixed lubrication are mixed three contact regimes which are, respectively the ridge-smooth plane direct contact, the conventional hydrodynamic lubrication and the physical adsorbed layer boundary lubrication and, respectively occur in different areas of the contact. The present mode of mixed lubrication belongs to the future mode of mixed lubrication defined by Zhang (2004b, 2006a, b) and is believed to be more engineering than the classical mode of mixed lubrication. The lubricant film pressure boundary conditions in the zone A shown in Fig. 2b are:

$$p|_{x=x_{be}} = 0 \quad p|_{zone\ A_1, x=x_{bl}} = p|_{zone\ A_2, x=x_{bl}} \quad (32)$$

Analysis for the lubrications, respectively occurring in the zone A_1 and the zone A_2 shown in Fig. 2b are demonstrated as follows.

Lubrication in the zone A_1: In the analysis of the lubrication in the zone A_1, the following assumptions are used:

- The lubricant in the zone A_1 is Newtonian;
- The lubricant viscosity follows the Barus viscosity equation (Barus, 1893);
- The operating condition is isothermal.

According to these assumptions, the compressible lubricant lubrication Reynolds equation in the zone A_1 is (Pinkus and Sternlicht, 1961):

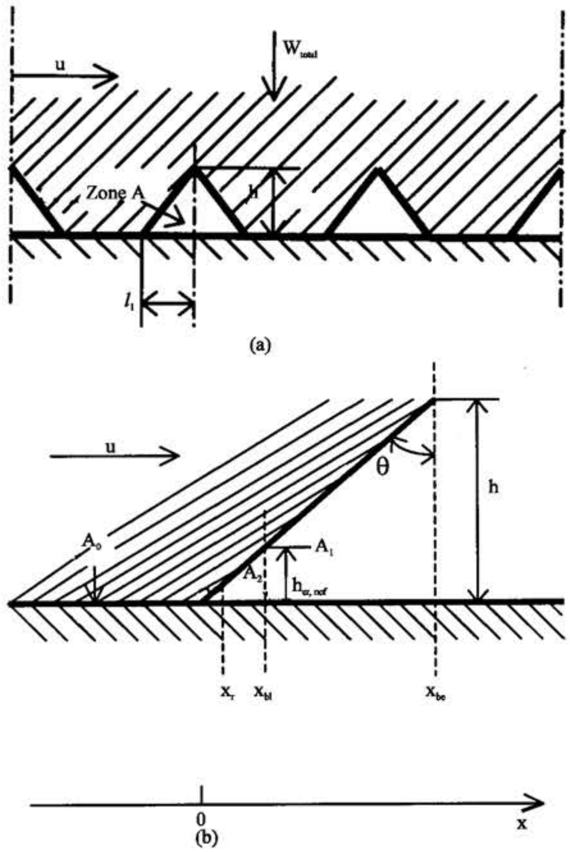

Fig. 2: The zone A in the present contact. (a) The geometry of the zone A for both types of surface ridges when the contact is loaded and (b) An elementary cell of the zone A and its geometries

$$\frac{\rho h_x^3}{\eta}\frac{dp}{dx} = 6u\rho h_x - 12q \tag{33}$$

where p is the lubricant film pressure, x is the coordinate shown in Fig. 2b, h_x is the lubricant film thickness at a coordinate x, ρ is the lubricant density, η is the lubricant viscosity and q is the lubricant mass flow through the contact.

Since the lubricant mass flow through the contact in the zone A_1 is equal to zero i.e., q = 0, Eq. 33 can be further simplified as:

$$h_x^2\frac{dp}{dx} = 6u\eta \tag{34}$$

Substituting $\eta = \eta_0 e^{\alpha p}$ (Barus, 1893) and $h_x = x\cot\theta$ into Eq. 34 and rearranging gives:

$$e^{-\alpha p}dp = \frac{\psi}{x^2}dx \tag{35}$$

where $\Psi = 6u\eta_0/\cot^2\theta$.

Integrating Eq. 35 and using the boundary condition $p|_{x=x_{be}} = 0$ gives the lubricant film pressure in the zone A_1:

$$p = -\frac{1}{\alpha}\ln\left(\frac{\alpha\psi}{x} + 1 - \frac{\alpha\psi}{x_{be}}\right) \tag{36}$$

where x_{be} is the x coordinate of the lubricant film entrance in the zone A_1 and $x_{be} = h\tan\theta$. The lubricant film pressure at the boundary $x = x_{bl}$ (Fig. 2b) is:

$$p|_{x=x_{bl}} = -\frac{1}{\alpha}\ln\left(\frac{\alpha\psi}{x_{bl}} + 1 - \frac{\alpha\psi}{x_{be}}\right) \tag{37}$$

where x_{bl} is the x coordinate of the boundary between the zone A_1 and the zone A_2 and $x_{bi} = h_{cr,ncf}\tan\theta$; Here, $h_{cr,ncf}$ is the critical thickness of the physical adsorbed layer boundary lubrication film. The load per unit contact length carried by the lubricant film in the zone A_1 on a single surface ridge is derived as:

$$w_{A_1,single} = \int_{x_{bl}}^{x_{be}} p\,dx = -\frac{\psi\ln x_{be}}{1-\frac{\alpha\psi}{x_{be}}} - x_{bl}p|_{x=x_{bl}} + \frac{\psi\ln[\alpha\psi + (1-\frac{\alpha\psi}{x_{be}})x_{bl}]}{1-\frac{\alpha\psi}{x_{be}}} \tag{38}$$

Lubrication in the zone A_2: Since the lubricant film thickness in the zone A_2 is of molecular scale, the zone A_2 is in physical adsorbed layer boundary lubrication. According to the physical adsorbed layer boundary lubrication theory developed by Zhang *et al.* (2003), Zhang and Lu (2005) and Zhang (2006c), the lubricant mass flow through the contact in the zone A_2 is equated as $q = q_{conv}\theta_v$, where q_{conv} is the lubricant mass flow through the contact in the zone A_2 when the boundary adsorbed layer in the zone A_2 is treated as the conventional continuous lubricant and θ_v is the correction factor of the lubricant mass flow through the contact in the zone A_2 due to the lubricant film discontinuity and inhomogeneity effects across the lubricant film thickness there. In the present analysis, since the lubricant mass flow q through the contact in the zone A_2 vanishes, $q_{conv} = 0$. In the zone A_2, due to the interaction between the lubricant molecule and the contact surfaces and the pressure within the lubricant film, the boundary adhering layer is solidified. In the present analysis, the shear modulus of elasticity and the Eyring stress of the boundary adhering layer (Zhang *et al.*, 2003) in the zone A_2 are not considered and the boundary adhering layer is assumed not to slip at the contact surfaces i.e., the shear strength at the contact surface-boundary adhering layer interface is assumed as large enough. In these conditions, the rheological model of the boundary adhering layer in the zone A_2 is simplified as (Zhang *et al.*, 2003; Zhang, 2004b):

$$\dot{\gamma} = \frac{\tau}{\eta_{ncf}^{eff}(p,h)} \tag{39}$$

where τ is shear stress, $\dot{\gamma}$ is shear strain rate and η_{ncf}^{eff} is the effective viscosity of the boundary adhering layer which is dependent on the pressure within and the thickness of the boundary adhering layer.

In the present analysis, the lubricant in the zone A_2 is taken as compressible and the operating condition is taken as isothermal. In these conditions and according to Eq. 39, the Reynolds equation for the boundary adhering layer in the zone A_2 is derived as (Zhang *et al.*, 2003):

$$\frac{\rho_{ncf}^{eff} h_x^3}{\eta_{ncf}^{eff}} \frac{dp}{dx} = 6u\rho_{ncf}^{eff} h_x - 12q_{conv} \tag{40}$$

where ρ_{ncf}^{eff} is the effective density of the boundary adhering layer. Since $q_{conv} = 0$, Eq. 40 can be further simplified as:

$$h_x^2 \frac{dp}{dx} = 6u\eta_{ncf}^{eff} \tag{41}$$

In Eq. 41, the viscosity is equated as (Zhang *et al.*, 2003):

$$\eta_{ncf}^{eff} = \eta_0 e^{\alpha p} C_y(h_x) \text{ for } r \le \frac{h_x}{h_{cr,ncf}} < 1 \tag{42}$$

where $C_y(h_x) = a_0 + a_1(h_x / h_{cr,ncf})^{-1} + a_2(h_x / h_{cr,ncf})^{-2}$ and r approaches zero.

Substituting Eq. 42 and $h_x = x\cot\theta$ into Eq. 41 and rearranging gives:

$$e^{-\alpha p}dp = \psi(a_0 x^{-2} + a_1 x^{-3} \cot^{-1}\theta\, h_{cr,ncf} + a_2 x^{-4} \cot^{-2}\theta\, h_{cr,ncf}^2)dx, \quad \text{for } r \le \frac{h_x}{h_{cr,ncf}} < 1 \tag{43}$$

Integrating Eq. 43 and using both the boundary condition formulated by Eq. 32 and the boundary pressure formulated by Eq. 37 gives the lubricant film pressure in the zone A_2 as follows:

$$p = -\frac{1}{\alpha}\ln[\alpha\psi a_0 x^{-1} + \frac{1}{2}\alpha\psi a_1 x^{-2} h_{cr,ncf} \cot^{-1}\theta + \frac{1}{3}\alpha\psi a_2 x^{-3} h_{cr,ncf}^2 \cot^{-2}\theta - \alpha C_\psi], \text{ for } r \le \frac{h_x}{h_{cr,ncf}} < 1 \tag{44}$$

where

$$C_\psi = \psi(a_0 - 1)/x_{bl} + \frac{1}{2}\psi a_1 x_{bl}^{-2} h_{cr,ncf} \cot^{-1}\theta + \frac{1}{3}\psi a_2 x_{bl}^{-3} h_{cr,ncf}^2 \cot^{-2}\theta - 1/\alpha + \psi / x_{be}$$

The load per unit contact length carried by the lubricant film in the zone A_2 on a single surface ridge is expressed as:

$$w_{A2,single} = \int_{x_r}^{x_{bl}} p\, dx \tag{45}$$

where x_r satisfies $r = h_x(x_r)/h_{cr,ncf}$.

Performance parameters

Load partition in the contact: Define the ratio of the carried load by the lubricant film lubricated area to that by the whole contact in the present modeled contact as:

$$R_w = \frac{w_{A1,single} + w_{A2,single}}{w_{A0,single} + w_{A1,single} + w_{A2,single}} \tag{46}$$

The value of R_w shows the load partition on the lubricant film lubricated area (or on the direct surface contact area between the two planes) in the present contact.

Total load: The load on the whole contact in the present contact is expressed as:

$$w_{total} = N(w_{A0,single} + w_{A1,single} + w_{A2,single}) \tag{47}$$

where N is the number of the surface ridge in the whole contact.

Let $w_{A0,\ total} = N\ w_{A0,\ single}$, $w_{A1,\ total} = N\ w_{A1,\ single}$ and $w_{A2,\ total} = N\ w_{A2,\ single}$. The parameters $w_{A0,\ total}$ $w_{A1,\ total}$ and $w_{A2,\ total}$ are the total loads, respectively on the direct surface contact area, the conventional hydrodynamic lubricated area and the physical adsorbed layer boundary lubrication area in the whole contact of the present model.

Load per unit contact width in the whole contact: Define the load per unit contact width in the whole contact as $w_{ul,\ total} = w_{total}/L$, where L is the initial width of the whole contact (before loading) (in the x coordinate direction, Fig. 2b". According to $N = L/l_w$, $l_w = 2h_0 \tan\theta$ and Eq. 47, the parameter $w_{ul,\ total}$ is equated as:

$$w_{ul,total} = \frac{w_{A0,single} + w_{A1,single} + w_{A2,single}}{2h_0 \tan\theta} \quad (48)$$

The parameter $w_{ul,\ total}$ can be used to study the influence of the initial rough contact surface geometry structure i.e., the surface ridge geometry shape parameter θ and the initial surface ridge height parameter h_0 on the mixed lubrication performance in the present model.

Total contact stiffness: The contact stiffness of the whole contact in the present model is expressed as:

$$Stf_{total} = N\left(\frac{\Delta w_{A0,single} + \Delta w_{A1,single} + \Delta w_{A2,single}}{\Delta h}\right) \quad (49)$$

Let $Stf_{A0,total} = N\Delta w_{A0,single}/\Delta h$, $Stf_{A1,total} = N\Delta w_{A1,single}/\Delta h$, and $Stf_{A2,total} = N\Delta w_{A2,single}/\Delta h$. The parameters $Stf_{A0,total}$, $Stf_{A1,\ total}$ and $Stf_{A2,total}$ are, respectively the contact stiffness of the total direct surface contact area, the total conventional hydrodynamic lubricated area and the total physical adsorbed layer boundary lubrication area in the whole contact.

In Eq. 49, $\Delta w_{A0,\ single}/\Delta h$ is expressed by Eq. 14, 18 or 30. The other two contact stiffness are, respectively expressed as follows:

$$\frac{\Delta w_{A1,single}}{\Delta h} = \begin{cases} 0 \quad , \text{ for } x_{bl} = x_{be} \\ t_1 \ln \dfrac{\alpha\psi + (1 - \dfrac{\alpha\psi}{x_{be}})x_{bl}}{x_{be}} + t_2\left(\dfrac{x_{bl}}{\alpha} + \dfrac{\psi x_{be}}{x_{be} - \alpha\psi}\right) \\ -\dfrac{\psi}{x_{be} - \alpha\psi}\tan\theta, \text{ otherwise} \end{cases} \quad (50)$$

where:

$t_1 = -\alpha\Psi^2 \tan\theta / (x_{be} - \alpha\Psi)^{2n}$

and $t_2 = \alpha\psi x_{bl} x_{be}^{-2} \tan\theta / [\alpha\psi + (1 - \alpha\psi/x_{be})x_{bl}]$

$$\frac{\Delta w_{A2,single}}{\Delta h} = -\frac{\psi}{\alpha} h^{-2} \tan^{-1}\theta \int_{x_r}^{x_{bl}} \frac{1}{\psi a_0 x^{-1} + \psi a_1 x^{-2} h_{cr,ncf} \cot^{-1}\theta / 2 + \psi a_2 x^{-3} h_{cr,ncf}^2 \cot^{-2}\theta / 3 - C_\psi} dx \quad (51)$$

CONCLUSIONS

The present study presents an analysis of an engineering mixed lubrication contact. In this contact, one contact surface is taken as rough, elastic-plastic and moving periodically imposed with regular ridges-isosceles triangle ridges or isosceles truncated triangle ridges; The other contact surface is taken as ideally smooth, rigid and stationary. The whole contact in the present model is composed of three types of contact areas i.e., the direct surface contact area between the contact surfaces, the conventional hydrodynamic lubricated area and the physical adsorbed boundary layer contact area; The direct surface contact area between the contact surfaces can be the oxidized chemical boundary layer contact area or the fresh metal-metal dry contact area. In this contact thus occurs mixed contact regimes. The present modeled contact is believed to be more engineering and realistic according to the experimental and theoretical research results.

Analysis are, respectively derived for the direct contact between the two planes, the conventional hydrodynamic lubricated area and the physical adsorbed boundary layer lubricated area in the present modeled contact, respectively for isosceles triangle surface ridges and isosceles truncated triangle surface ridges when the contact is loaded. The load-carrying capacity and contact stiffness of the present contact are obtained. In the following parts will be presented in detail the results obtained from the present analysis, respectively for isosceles triangle surface ridges and isosceles truncated triangle surface ridges.

Nomenclature

A = Area of the contact formed between a single ridge and the ideally smooth rigid plane

A_{org} = Initial direct contact area between a single truncated triangle ridge and the smooth plane, $2b_0 l$

b_0 = Initial half width of the direct contact between a single truncated triangle ridge and the smooth plane
c_0, c_1 = Integral constants
c_m = Specific heat of the rough surface
C_y = Function of film thickness, Eq. 42
f = Friction coefficient of the ridge-plane direct contact area
F = Force exerted on the whole area of the contact between a single ridge and the ideally smooth rigid plane
h = Film thickness between the root of the ridge and the smooth plane
$h_{cr,e}$ = (critical) value of the film thickness h when the ridge is in the maximum elastic deformation
$h_{cr,ncf}$ = Critical thickness of the physical adsorbed layer boundary lubrication film
h_x = Lubricant film thickness at a coordinate x
h_0 = Initial height of the ridge
k = Constant
k_m = Heat conduction coefficient of the rough surface
l = Contact length of the ridge
l_w = Initial wavelength of the contact surface roughness
l_1 = Width of the zone A shown in Fig. 2a
L = Initial contact width of the rough surface (before loading)
N = Number of the surface ridge in the whole contact
p = Lubricant film pressure
p_{av} = Average pressure formed on the direct surface contact area between the ridge and the smooth plane
p_y = Compressive yielding strength of the ridge
q = Lubricant mass flow through the contact
q_{conv} = Lubricant mass flow through the contact in the zone A_2 shown in Fig. 2b when the boundary adsorbed layer in that zone is treated as the conventional continuous lubricant
R_w = Ratio of the carried load by the lubricant film lubricated area to that by the whole contact in the present modeled contact
$Stf_{A0,\ total}$ = $N\Delta w_{A0,\ single}/\Delta h$
$Stf_{A1,\ total}$ = $N\Delta w_{A2,\ single}/\Delta h$
$Stf_{A2,\ total}$ = $N\Delta w_{A2,\ single}/\Delta h$
Stf_{total} = Contact stiffness of the whole contact in the present model
u = Sliding speed between the contact surfaces
$w_{A0,single}$ = Load per unit contact length on the direct surface contact area between a single ridge and the smooth plane, F/l
$w_{A1,single}$ = Load per unit contact length carried by the lubricant film in the zone A_1 on a single surface ridge shown in Fig. 2b
$w_{A2,single}$ = Load per unit contact length carried by the lubricant film in the zone A_2 on a single surface ridge shown in Fig. 2b
$w_{max,e}$ = Maximum load on the direct surface contact area between a single ridge and the smooth plane when the ridge undergoes elastic deformation
w_{total} = Load on the whole contact in the present contact
$w_{ul,\ total}$ = Load per unit contact width in the whole contact
x = Coordinate shown in Fig. 2b
x_{be} = x coordinate of the lubricant film entrance in the zone A_1 shown in Fig. 2b
x_{bl} = x coordinate of the boundary between the zone A_1 and the zone A_2 shown in Fig. 2b
θ = Half ridge angle
θ_v = Correction factor of the lubricant mass flow through the contact in the zone A_2 shown in Fig. 2b due to the lubricant film discontinuity and inhomogeneity effects across the lubricant film thickness (Zhang and Lu, 2005; Zhang, 2006)
ρ = Lubricant density
ρ_m = Density of the rough surface
ρ_{ncf}^{eff} = Effective density of the boundary adhering layer
η = Lubricant viscosity
η_0 = Viscosity of continuum lubricant at ambient condition
η_{ncf}^{eff} = Effective viscosity of the boundary adhering layer
α = Viscosity-pressure index of lubricant
τ = Shear stress
$\dot{\gamma}$ = Shear strain rate
Ψ = $6u\eta_0/\cot^2\theta$
ΔT = Temperature rise of the direct contact area between the ridge and the smooth plane
$Stf_{A0,\ total}$, $Stf_{A1,\ total}$, $Stf_{A2,\ total}$ = Contact stiffness of the total direct surface contact area, the total conventional hydrodynamic lubricated area and the total physical adsorbed layer boundary lubrication area in the whole contact
$w_{A0,\ total}$, $w_{A1,\ total}$, $w_{A2,\ total}$ = Total loads, respectively on the direct surface contact area, the conventional hydrodynamic lubricated area and the physical adsorbed layer boundary lubrication area in the whole contact of the present model

REFERENCES

Barus, C., 1893. Am. J. Sci., 45: 87-93.

Begelinger, A. and A.W.J. Gee de, 1974. Thin film lubrication of sliding point contacts of AISI 52100 steel. Wear, 28: 103-114.

Begelinger, A. and A.W.J. Gee de, 1976. On the mechanism of lubricant film failure in sliding concentrated steel contacts. J. Lubri. Tech., 98: 575-579.

Blok, H., 1937. General discussion on lubrication. Proc. Instn. Mech. Eng., 14: 222-235.

Christensen, H., 1969-1970. Stochastic models for hydrodynamic lubrication of rough surfaces. Proc. Instn. Mech. Engrs., 184: 1013.

Christensen, H. and K. Tonder, 1969. Tribology of rough surfaces-Stochastic models of hydrodynamic lubrication. SINTEF Report 18-69/10, Trondheim, Norway.

Goglia, P.R., T.F. Conry and C. Cusano, 1984. The effects of surface irregularities on the elastohydrodynamic lubrication of sliding line contacts: Part I-Single irregularities. ASME JOT., 106: 104-112.

Greenwood, J.A. and K.L. Johnson, 1992. The behavior of transverse roughness in sliding elastohydrodynamically lubricated contacts. Wear, 153: 107-117.

Holmes, M.J.A., H.P. Evans, T.G. Hughes and R.W. Snidle, 2003. Transient elastohydrodynamic point contact analysis using a new coupled differential deflection method Part 2: Results. Proc. Instn. Mech. Eng. Part J: J. Eng. Trib., 217: 305-322.

Hughes, G.D. and A.W. Bush, 1993. An average Reynolds equation for non-Newtonian fluids in EHL line contacts. ASME JOT., 115: 666-669.

Hu, Y.Z. and D. Zhu, 2000. A full numerical solution to the mixed lubrication in point contacts. ASME JOT., 122: 1-9.

Jiang, X., D.Y. Hua, H.S. Cheng, X. Ai and S.C. Lee, 1999. Mixed elastohydrodynamic lubrication model with asperity contact. ASME JOT., 121: 481-491.

Lubrecht, A.A., W.E. Napel and R. Bosma, 1988. The influence of longitudinal and transverse roughness on the elastohydrodynamic lubrication of circular contacts. ASME JOT., 110: 421-426.

Patir, N. and H.S. Cheng, 1979. Application of average flow model to lubrication between rough sliding surfaces. J. Lubri. Tech., 101: 220-230.

Pinkus, O. and B. Sternlicht, 1961. Theory of Hydrodynamic Lubrication, McGraw-Hill Book Company, Inc., New York.

Tabor, B.J., 1981. Failure of thin film lubrication-an expedient for the characterization of lubricants. J. Lubri. Tech., 103: 497-501.

Timoshenko, S. and J.N. Goodier, 1951. Theory of Elasticity, McGraw-Hill Book Company, Inc., New York.

Zhang, Y.B., K. Tang and G.S. Lu, 2003. Model of elastohydrodynamic lubrication with molecularly thin lubricating films: Part I-Development of analysis. Int. J. Fluid Mech. Res., 30: 542-557.

Zhang, Y.B., 2004a. Review of mixed lubrication in concentrated contacts: Thinning, mixed and partial films, classical, modern and future modes. submitted to Industr. Lubri. Trib

Zhang, Y.B., 2004b. Modeling of elastohydrodynamic lubrication with molecularly thin lubricating films. J. Balkan Tribol. Assoc., 10: 394-421.

Zhang, Y.B., 2005a. How does dry contact occur in elastohydrodynamic lubrication. Industr. Lubri. Trib., 57: 176-180.

Zhang, Y.B., 2005b. A justification of the load-carrying capacity of elastohydrodynamic lubrication film based on the Newtonian fluid model. Industr. Lubri. Trib., 57: 224-232.

Zhang, Y.B. and Lu, G.S., 2005c. Flow factor for molecularly thin fluid films in one-dimensional flow due to fluid discontinuity. J. Mol. Liq., 116: 43-50.

Zhang, Y.B., 2006a. Boundary lubrication-An important lubrication in the following time. J. Mol. Liq., 128: 56-59.

Zhang, Y.B., 2006b. Contact-fluid interfacial slippage in hydrodynamic lubricated contacts. J. Mol. Liq., 128: 99-104.

Zhang, Y.B., 2006c. Flow factor of non-continuum fluids in one-dimensional contact. Industr. Lubri. Trib., 58: 151-169.